Engineering Journal issn: 0125-8281

Article

Electronic and Ionic Conductivities Enhancement of Zinc Anode for Flexible Printed Zinc-Air Battery

Jutamart Chotipanich[1], Amornchai Arpornwichanop[1], Tetsu Yonezawa[2], and Soorathep Kheawhom[1,*]

1 Computational Process Engineering Research Laboratory, Department of Chemical Engineering, Faculty of Engineering, Chulalongkorn University, Bangkok 10330, Thailand
2 Division of Materials Science and Engineering, Faculty of Engineering, Hokkaido University, Kita 13 Nishi 8, Sapporo, Hokkaido 060-8628, Japan
*E-mail: soorathep.k@chula.ac.th (Corresponding author)

Abstract. Zinc-air batteries are considered promising energy storage devices for future energy applications due to their high energy density, safety, and low cost. However, poor battery performance and low efficiency of zinc utilization, resulted from passivation effect of the zinc anode, is a major challenge. Thus, in this work, investigation of electronic and ionic conductivities enhancement of the zinc anode for flexible printed zinc-air batteries has been carried out. The anode was made from zinc-based inks, prepared from a mixture of zinc and zinc oxide particles. Carbon black, sodium silicate (Na_2SiO_3) and bismuth oxide (Bi_2O_3) were investigated for implementation on the anode. The results showed that performance of the batteries increased when carbon black was introduced into the anode as the presence of carbon black improved electronic conductivity of the anode. Again, the batteries performed better when Bi_2O_3 or Na_2SiO_3 was introduced due to the formation of solid electrolyte interface(SEI) on the anode. The SEI inhibits passivation of zinc active surfaces and provides effective electrolyte access. The batteries with Bi_2O_3 provided the best performance. The highest performance was observed when Bi_2O_3 content reached 26 wt.%. No significant improvement was observed when Bi_2O_3 concentration increased higher than 26 wt.%.

Keywords: Zinc-air battery, screen printing, thin film, ionic conductivity, electronic conductivity.

ENGINEERING JOURNAL Volume 22 Issue 2
Received 31 May 2017
Accepted 20 December 2017
Published 30 March 2018
Online at http://www.engj.org/
DOI:10.4186/ej.2018.22.2.47

DOI:10.4186/ej.2018.22.2.47

1. Introduction

Recently, fabrication of electronic devices and batteries using printing techniques has received increasing attention because of its simplicity, high throughput and environmental friendliness [1, 2, 3, 4, 5, 6]. Furthermore, printing techniques allow the manufacture of flexible and low-cost devices. Different types of flexible batteries have been successfully fabricated by printing techniques e.g. zinc-manganese oxide battery [7, 8], lithium-ion battery [9], zinc-silver battery [10] and zinc-air battery [11].

Zinc-air batteries are attractive as a power source for many applications [12, 13, 14]. These batteries use relatively safe and low-cost raw materials, but exhibit high specific energy density. Besides, zinc has low toxicity and is environmentally friendly.

Main components of zinc-air batteries include zinc anode and air cathode. The zinc anode significantly affects zinc utilization and performance of the batteries. Recently, the anode made of zinc particles becomes more attractive because of its higher effective surface area which is an important factor determining performance of the batteries [15]. However, passivation of zinc active surfaces by zinc oxide (ZnO) layers generated during discharge restricts the efficiency of zinc utilization [16]. Thus, various synthesis and fabrication methods have been proposed, and different additives were introduced to improve the electrochemical performance of the batteries [17, 18, 19, 20, 21]. These additives must be inert but provide enhancement of electronic conductivity with excellent inter-particle contact and offer optimal electrolyte access.

Li et al. [22] reported that electronic conductivity of the cathode increased with carbon black content. Hilder et al. [23] employed carbon powder as physical bridges to connect isolated zinc particles in polycarbonate films. Also, Hilder et al. [24] reported that additive carbon, functioning as a conductive link between isolated zinc particles in a porous zinc anode, considerably improves performance of the batteries. The addition of graphite powder into an anode was studied [25]. However, this study reported that the graphite blocks the zinc particles and hinders the electrolyte access. Thus, the battery capacity dropped proportionally with increasing of the graphite content and reached its limit at 10 wt.% graphite content. Later, the effects of carbon black additive in the zinc-air batteries were investigated [13]. It was found that the introduction of carbon black remarkably enhanced the electrochemical performance of the batteries because the carbon particles act as conductive bridges connecting between zinc particles.

As it was previously mentioned that the zinc anode prepared from zinc particles offer several advantages for the batteries. Various types of binders or gels have been used to fabricate the zinc anode. The binders bind all active material particles together and prevent them from disintegrating. Poly(tetrafluoroethylene) (PTFE) was used in a zinc/air fuel cell [26]. High ionic conducting polymer electrolyte prepared from poly(vinyl alcohol)(PVA) and poly(acrylic acid) (PAA) was implemented in the zinc-air batteries [27]. Tapioca was also used as a binder for a porous zinc anode in the zinc-air batteries [28]. It was reported that higher utilization of the zinc particles could be achieved indicating that tapioca acts as a good binder. Hilder et al. [24] reported that by using sodium silicate (Na_2SiO_3) instead of poly(carbonate) as a binder, the performance of the zinc-air batteries in terms of conductivity and efficiency of the anode were considerably improved. The porous nature of Na_2SiO_3 binder allows easy penetration of the electrolyte. Na_2SiO_3 was reported to help minimizing the passivation film on zinc active surfaces created during discharge thus improving discharge capacity of the zinc anode. Moreover, it was reported that Na_2SiO_3 increases the solubility of ZnO in alkaline electrolytes [29]. Bismuth oxide (Bi_2O_3) has been introduced to improve ionic conductivity for both cathode and electrolyte [30]. A carbon coated Bi_2O_3 nanoparticles/nitrogen-doped reduced graphene oxide was reported as a high performance anode for lithium-ion batteries [31]. Moreover, the addition of Bi_2O_3 has been reported for its effectiveness and simplicity in improving cycling performance of the zinc anode [32]. Previous studies suggested that the enhanced cycle performance resulted from the advanced electrical conductivity [33, 34]. However, in comparison with conductive carbon powder, Bi_2O_3 is not the most effective additive to promote the electrical conductivity. Shin et al. [32] suggested that the absorption of zincate ions, produced during discharge of zinc-ion batteries, on the surface of bismuth species helps to improve electrochemical performance of the batteries .Our previous work has successfully fabricated flexible printed zinc-air batteries using a screen printing technique [11]. In this work, further improvement of the batteries is carried out by improving electronic and ionic conductivities of the zinc anode. Three types of additive materials (carbon black, Na_2SiO_3 and Bi_2O_3) were investigated. Carbon black was used to improve electronic conductivity while Na_2SiO_3 and Bi_2O_3 were implemented to improve ionic conductivity and to hinder passivation of the zinc active surfaces. The effects of these additives on characteristic and performance of the batteries were studied.

2. Experimental Details

Commercial nano-silver ink (NovaCentrix, 75%) was used to fabricate both the anode and cathode current collectors. Zinc powder (Ajax Finechem Pty. Ltd, 99.9%), ZnO particles (QReC, 99%), styrene-butadiene binder (SBD, Sigma-Aldrich PTE Ltd., 5%), sodium silicate (Na_2SiO_3, Sigma-Aldrich PTE Ltd., 5% liquid glass solution) and bismuth oxide (Bi_2O_3, QReC, 99.5%) were used to prepare the anodes. Polyethylene terephthalate(PET) was used as the anode substrate. Carbon black (20 μm particles size, Sigma-Aldrich PTE Ltd.) was used in fabrication of the cathodes and anodes. Toluene (QReC, 99.8%) was used as the solvent for preparing zinc and carbon black based inks for the anodes and cathodes, respectively. Polypropylene membrane (0.45 μm pore sizes, Sigma-Aldrich PTE Ltd.) was used as the air cathode substrate and separator. KOH (QReC) was used to prepare the electrolyte. Methyl ethyl ketone (Ajax Finechem Pty. Ltd.) was used to seal the border of the fabricated batteries. All chemicals were used without further purification.

The anode current collectors were fabricated by screen-printing nano-silver ink on a PET substrate and annealing at 120 ◦C for 1 h. Zinc-based functional ink was prepared by mixing 1 g zinc powder, 0.1053 g ZnO particle, 0.0231 g styrene-butadiene binder and 4 g toluene solvent. ZnO was added to suppress corrosion of the anodes. The zinc-based ink was then printed onto the anode current collectors using screen-printing and annealed at 70 ◦C for 1 h. To prepare zinc/carbon (Zn/C) ink, 0.7144 g carbon black was mixed with zinc-based ink. To investigate the effects of Na_2SiO_3 and Bi_2O_3, 0.0183 g Na_2SiO_3 or 0.7144 g Bi_2O_3 were mixed with Zn/C ink, respectively. In the case of investigating Na_2SiO_3 which also functioned as a binder, the Zn/C ink was prepared by using deionized water as the solvent without the insoluble styrene-butadiene binder. Also, 2.05 g and 2.75 g Bi_2O_3 were used to fabricate the anodes to investigate the effects of Bi_2O_3 content.

The electrical resistivity of the anodes was measured by the van der Pauw method using a 4-point probe (Keithley Instruments, 2182A digital nanovoltmeter). The crystalline structure of the zinc anodes was analyzed by X-ray diffractometer (XRD; Bruker, D2 PHASER) operating in the reflection mode using Cu Kα radiation. The morphologies of the anodes were analyzed by Field Emission Scanning Electron Microscope (FESEM; JEOL, JSM-5800LV) operated at 15.0 kV.

The cathode current collectors were prepared by screen-printing nano-silver ink on polypropylene membrane substrate and annealing at 120 ◦C for 1 h. The cathodes were fabricated by screen-printing carbon black ink, prepared by mixing 1.0 g carbon black, 0.1320 g styrene butadiene binder and 2 g of toluene solvent, on top of the cathode current collectors and annealed at 70 ◦C for 1 h. 0.1 mL of 9 M KOH solution in deionized water used as the electrolyte was dropped onto the anodes. Subsequently, a polypropylene separator was immersed in 9 M KOH solution for 5 min. The batteries were fabricated by laminating the separator between the cathodes and the anodes. The borders of the batteries were sealed by methyl ethyl ketone.

Battery performance was determined by battery analyzer (Battery Metric, MC2020). The polarization curve of each battery was determined using five experiments on five independent samples. The polarization curve was obtained by varying the discharge current density in the range of 0-10 mA/cm^2. The batteries were also discharged at constant current density at 1 or 2 mA/cm^2. The area under each voltage-time discharge curve is proportional to total energy that the batteries delivered. In comparison, the voltage profile is proportional to power of the batteries. The energy density was calculated from multiplication of the area under the curve and the discharge current density. The power density was estimated from multiplication of the average voltage and the discharge current density. Moreover, electrochemical impedance spectroscopy (EIS) measurement was performed using a potentiostat/galvanostat with impedance measurement unit (AMETEK, PAR VersaSTAT 3A). The EIS measurements were carried out at a DC discharge current density of 2 mA/cm^2 with an AC excitation signal of 10mV. in the frequency range of 10^{-1} to 10^5 Hz.

3. Results and Discussion

Figure 1(a) shows a cross-sectional diagram of the zinc-air batteries. Zinc is the anode active material. The dissolution of zinc involves two steps. The oxidation of zinc to zincate ion ($Zn(OH)_4^{2-}$) occurs in the first step. $Zn(OH)_4^{2-}$ is soluble in an aqueous alkaline electrolyte.

$$Zn + 4OH^- \longrightarrow Zn(OH)_4^{2-} + 2e^-$$

After that, precipitation of zinc oxide (ZnO) takes place when the dissolved $Zn(OH)_4^{2-}$ reaches its solubility limit.

$$Zn(OH)_4^{2-} \longrightarrow ZnO + H_2O + 2OH^-$$

At the anode, zinc and hydroxide ion (OH^-), supplied from the electrolyte, are consumed. Simultaneously, ZnO and water (H_2O) are produced.

$$Zn + 2OH^- \longrightarrow ZnO + H_2O + 2e^-$$

During discharge over time, zinc particles in the anode upon oxidation generate $Zn(OH)_4^{2-}$. $Zn(OH)_4^{2-}$ dissolves in an alkaline electrolyte and relaxes into ZnO. ZnO, precipitated from supersaturated $Zn(OH)_4^{2-}$ at the surface of zinc particles, forms a loose and porous inactive layer. Though this layer does not completely block the surface of zinc particles, it impedes OH^- and $Zn(OH)_4^{2-}$ transport [35]. Besides, at high current density and supersaturated $Zn(OH)_4^{2-}$, zinc can directly change into ZnO film. This oxide film behaves as a barrier for further dissolution of the zinc particles [36].

Oxygen (O2) from atmospheric air is the cathode active material. At the cathode, the oxygen reduction reaction (ORR) consumes O_2 and H_2O and simultaneously produces OH^-. Thus, OH^-generated at the cathode transports through the separator and makes up OH^- consumed at the anode. In contrast, H_2O produced at the anode transfers across the separator and replenishes H_2O consumed at the cathode.

$$O_2 + 2H_2O + 4e^- \longrightarrow 4OH^-$$

Figure 1(b) shows a photographic image of the fabricated batteries. The dimension of the batteries is 2.5 cm × 2.5 cm with a total thickness of 0.8 mm. The active area of the batteries is 6.25 cm^2.

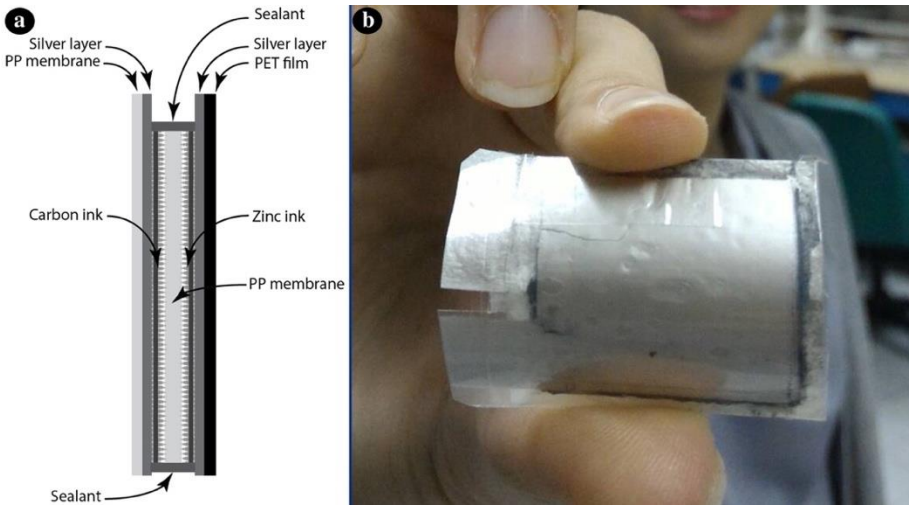

Fig. 1. (a) cross-sectional diagram of the zinc-air batteries and (b) photographic image of the fabricated batteries.

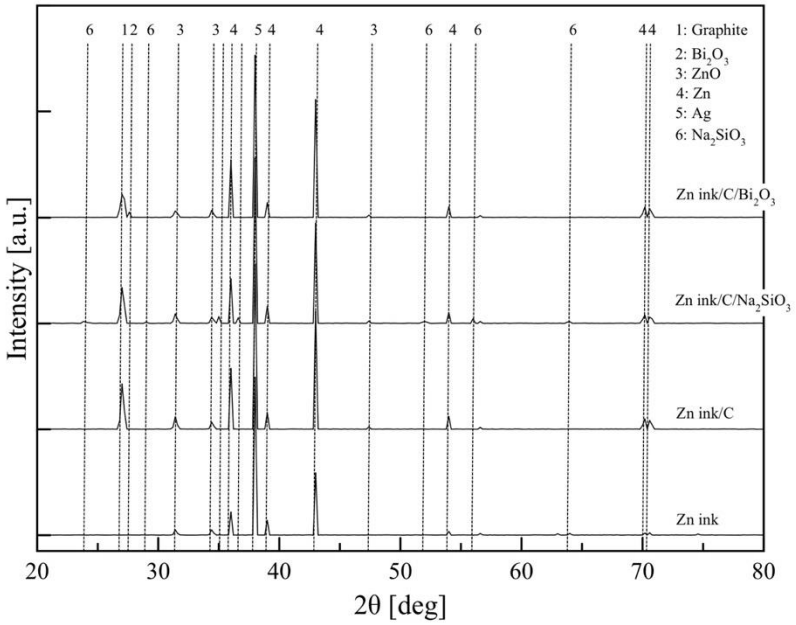

Fig. 2. XRD patterns of the anodes: Zn ink (88.62 Zn, 9.33 ZnO, 2.04 SBD, wt.% dry basis), Zn ink/C (54.26Zn, 5.71 ZnO, 1.25 SBD, 38.77 C, wt.% dry basis), Zn ink/C/C/Na_2SiO_3(54.41 Zn, 5.73 ZnO, 38.87 C, 1.00Na_2SiO_3, wt.% dry basis) and Zn ink/C/C/Bi_2O_3(39.10 Zn, 4.12 ZnO, 0.90 SBD, 27.94 C, 27.94 Bi2O3, wt.%dry basis).

The zinc anodes printed on top of the anode current collectors were characterized using XRD analysis. The XRD patterns are depicted in Fig. 2. The patterns were compared with the peaks reported by Joint Committee on Power Diffraction Standards (JCPDS). In all cases, the patterns confirm that the anodes contain high crystallinity of silver and zinc. The patterns also confirm the presence of additives (carbon black, Na_2SiO_3 and Bi_2O_3). Moreover, the products of a reaction between zinc and additives were not detected.

FESEM images of the zinc anodes with various additives are shown in Fig. 3. Figure 3(a) clearly shows that zinc particles deposited on the anode without additives are not well contacted and do not form contiguous electrical pathways throughout the surface, thus providing poor electrical conductivity. In addition, during discharge, ZnO, which is a discharge product, is formed at the surfaces of zinc particles resulting in further decreasing of electrical conductivity as ZnO is not a good electrical conductor. Figure 3(b) shows the FESEM image of the zinc anode mixed with carbon black. As shown in the figure, carbon flakes are observed. These carbon flakes act as conductive bridges to connect the isolated zinc particles resulting in improvement of electrical conductivity of the anode. Moreover, during discharge, though nonconductive ZnO is formed, carbon flakes function as conductive pathways and help stabilizing electrical conductivity of the anode. Figure 3(c) shows the FESEM image of the zinc anode mixed with carbon black and Na_2SiO_3. Na_2SiO_3 functions as a binder holding all particles together. A matrix of Na_2SiO_3 as well as carbon flakes are observed. In Fig. 3(d), zinc-based ink was mixed with carbon black and Bi_2O_3. The FESEM image shows small particles of Bi_2O_3 distributed over zinc particles. In addition, carbon flakes can be noticed.

DOI:10.4186/ej.2018.22.2.47

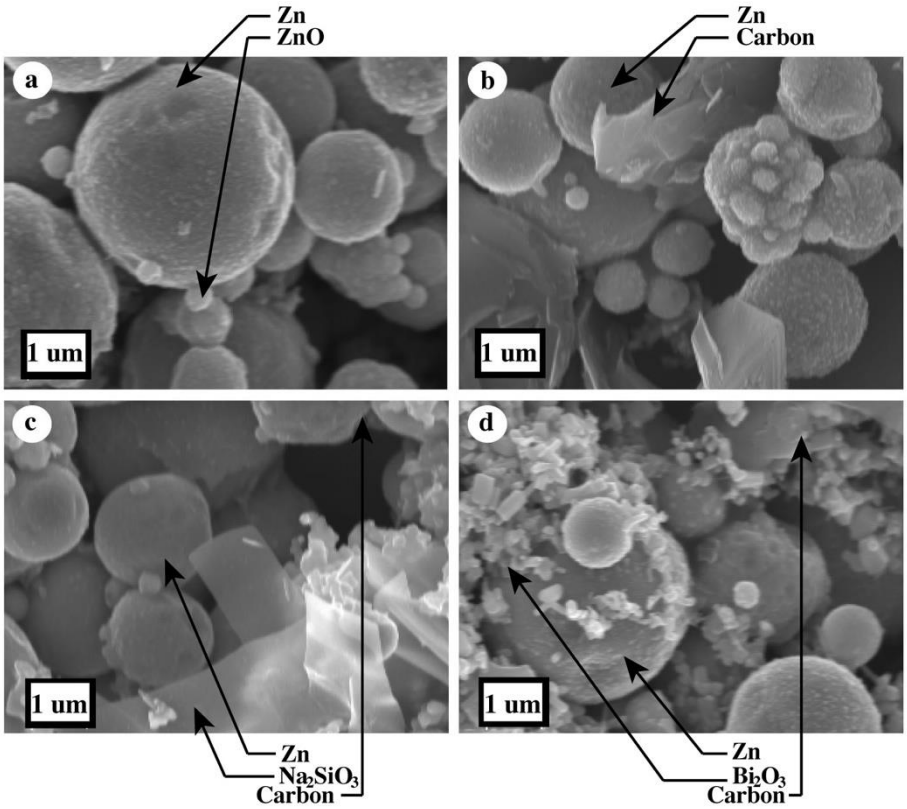

Fig. 3. FESEM images of the zinc anodes with various additives: (a) without additives (88.62 Zn, 9.33 ZnO, 2.04 SBD, wt.% dry basis), (b) carbon black (54.26 Zn, 5.71 ZnO, 1.25 SBD, 38.77 C, wt.% dry basis), (c) carbon black/Na2SiO3 (54.41 Zn, 5.73 ZnO, 38.87 C, 1.00 Na_2SiO_3, wt.% dry basis) and (d) carbon black/Bi_2O_3 (39.10 Zn, 4.12 ZnO, 0.90 SBD, 27.94 C, 27.94 Bi_2O_3, wt.% dry basis).

Table 1. Electrical resistivity and EIS parameters of the batteries: No additives (88.62 Zn, 9.33 ZnO, 2.04 SBD, wt.% dry basis), C (54.26 Zn, 5.71 ZnO, 1.25 SBD, 38.77 C, wt.% dry basis), C/Na_2SiO_3 (54.41 Zn, 5.73 ZnO, 38.87 C, 1.00 Na_2SiO_3, wt.% dry basis) and C/Bi_2O_3 (39.10 Zn, 4.12 ZnO, 0.90 SBD, 27.94 C, 27.94 Bi_2O_3, wt.% dry basis).

	Anode resistivity (Ω/□)	**R_e (Ω/cm²)**	**R_{ct} (Ω/cm²)**
No additives	0.0154	1.46	4.40
C	0.0122	0.81	3.24
C/Na_2SiO_3	0.0362	0.91	2.41
C/Bi_2O_3	0.0125	0.82	1.94

Table 1 shows the sheet resistance of the anodes using various additives. The resistance of the anode without additional conductive materials was 0.0154 Ω/□. The resistance of the anode decreased when zinc-based ink was mixed with carbon black (Zn/C) as the introduced carbon flakes provide conductive pathways to connect the isolated zinc particles. Mixing Zn/C based ink with Bi_2O_3 did not affect significantly the electrical resistance of the anode. However, when Zn/C based ink was mixed with Na_2SiO_3, the electrical resistance of the anode slightly increased because Na_2SiO_3 has low electrical conductivity.

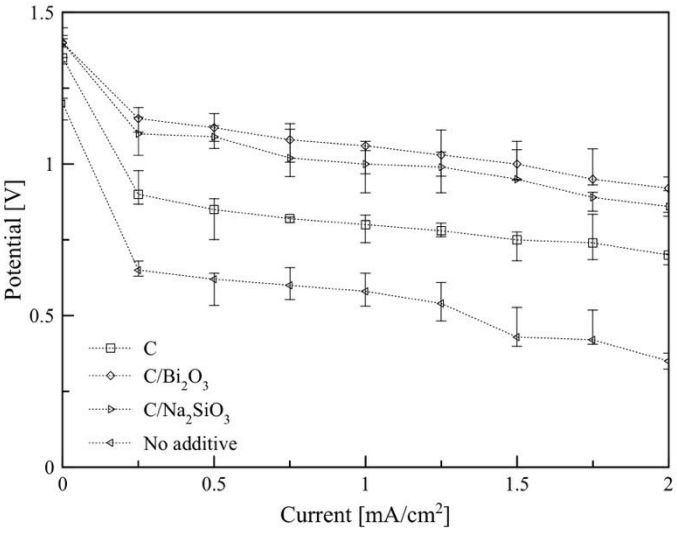

Fig. 4. Polarization curves of the batteries with various additives: No additives (88.62 Zn, 9.33 ZnO, 2.04 SBD, wt.% dry basis), C (54.26 Zn, 5.71 ZnO, 1.25 SBD, 38.77 C, wt.% dry basis), C/Na_2SiO_3 (54.41 Zn, 5.73 ZnO, 38.87 C, 1.00 Na_2SiO_3, wt.% dry basis) and C/Bi_2O_3 (39.10 Zn, 4.12 ZnO, 0.90 SBD, 27.94 C, 27.94 Bi_2O_3, wt.% dry basis).

Figure 4 shows the polarization curves of the batteries with various additives. The performance of the battery without additive was the lowest. During discharge, zinc transforms to $Zn(OH)_4^{2-}$. $Zn(OH)_4^{2-}$ further relaxes into ZnO depositing on the surfaces of zinc particles. ZnO has much lower conductivity in comparison to zinc. Moreover, ZnO impedes the transport of OH^- and $Zn(OH)_4^{2-}$ or partially passivates the zinc active surfaces by blocking electrolyte access. By mixing the zinc-based ink with carbon black, the performance of the batteries significantly enhanced. The added carbon flakes provide effective conductive pathways for the anode. By introducing Na_2SiO_3 or Bi_2O_3, the performance of the batteries was significantly enhanced although these additives have small effects on electrical resistance of the anode, as reported in Table 1. This issue is further discussed using EIS data.

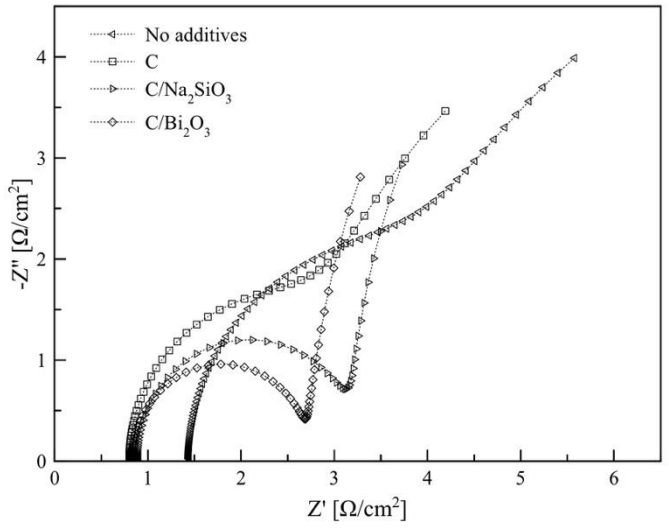

Fig. 5. Nyquist plots for electrochemical impedance spectroscopy of the batteries: No additives (88.62 Zn, 9.33 ZnO, 2.04 SBD, wt.% dry basis), C (54.26 Zn, 5.71 ZnO, 1.25 SBD, 38.77 C, wt.% dry basis),C/Na_2SiO_3 (54.41 Zn, 5.73 ZnO, 38.87 C, 1.00 Na_2SiO_3, wt.% dry basis) and C/Bi_2O_3 (39.10 Zn, 4.12 ZnO, 0.90 SBD, 27.94 C, 27.94 Bi_2O_3, wt.% dry basis).

Figure 5 presents the Nyquist plot of EIS data of the batteries with different additives at a current density of 2 mA/cm². The EIS data present two overlapping semicircles with one in the high frequency area and a sloping line in the low frequency area. The first interception at the high frequency end, represents the sum of ohmic resistance (R_e) of each cell. The semicircle at high frequency is associated with an interfacial capacitance and a charge transfer resistance (R_{ct}). The value of R_{ct} of each case was approximated by fitting the EIS data to an equivalent circuit model. The estimated EIS parameters are shown in Table 1. The battery without additives has the largest R_{ct}, while the R_{ct} of the battery with Bi_2O_3 is lower than others. The smaller R_{ct} indicates that the electrode surface reaction process is faster, which has beneficial effects on the performance of the batteries. In other words, the increase in charge transfer resistance leads to a slow zinc dissolution rate. The results suggested that carbon black effectively reduces the ohmic resistance of the batteries. In addition, the presence of Na_2SiO_3 and Bi_2O_3 in the anode further enhanced the performance of the batteries by reducing the charge transfer resistance. Adsorption of Na_2SiO_3 or Bi_2O_3 on zinc particles forms solid electrolyte interface (SEI) on the zinc particles and hinders direct precipitation of ZnO but allows penetration of the electrolyte to the zinc active surfaces. Besides, Na_2SiO_3 helps enhancing the solubility of ZnO [29] by suppressing precipitation of ZnO at the surfaces of zinc particles. Both additives have favorable effects on performance of the batteries.

The results agree with the results reported by Hilder et al. [24] that the performance of the batteries can significantly be enhanced by replacing polycarbonate binder with sodium silicate binder. Although, both Na_2SiO_3 and Bi_2O_3 could enhance the performance of the batteries, however, the performance of the battery using Na_2SiO_3 was lower than that of Bi_2O_3 because adding Bi_2O_3 did not adversely affect electrical conductivity, as Na_2SiO_3, as shown in Table 1. Bi_2O_3 improved ionic conductivity of the anode and inhibited passivation of zinc particles [37] by facilitating the transport of hydroxide ions across multilayers of zinc particles, including those which do not directly make contact with the electrolyte.

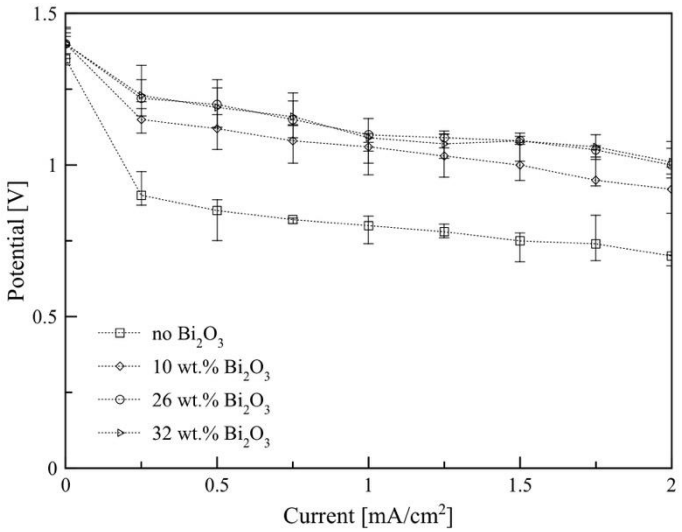

Fig. 6. Polarization curves of the batteries using carbon black and various wt.% of Bi_2O_3: no Bi_2O_3 (54.26 Zn, 5.71 ZnO, 1.25 SBD, 38.77 C, wt.% dry basis), 10 wt.% Bi_2O_3 (39.10 Zn, 4.12 ZnO, 0.90 SBD, 27.94 C, 27.94 Bi_2O_3, wt.% dry basis), 26 wt.% Bi_2O_3 (25.69 Zn, 2.70 ZnO, 0.59 SBD, 18.35 C, 52.66 Bi_2O_3, wt.% dry basis) and 32 wt.% Bi_2O_3 (21.77 Zn, 2.29 ZnO, 0.50 SBD, 15.55 C, 59.88 Bi_2O_3, wt.% dry basis).

Figure 6 shows the polarization curves of the batteries with carbon black and Bi_2O_3 at various concentrations. It is shown that when Bi_2O_3 content in zinc-based ink was increased, the batteries exhibited slightly higher potential especially at high current density. However, the batteries with 26 wt.% and 36 wt.% Bi_2O_3 showed similar characteristics. Beyond 26 wt.% Bi_2O_3, significant improvement of the batteries was not observed. Excessive loading of Bi_2O_3 does not benefit electrochemical performance of the batteries because Bi_2O_3 does not take part in zinc dissolution reaction but only form SEI layer on zinc active surfaces.

Moreover, excessive loading of Bi_2O_3 may result in adverse effects to the performance of the batteries as it reduces the zinc content in the anode.

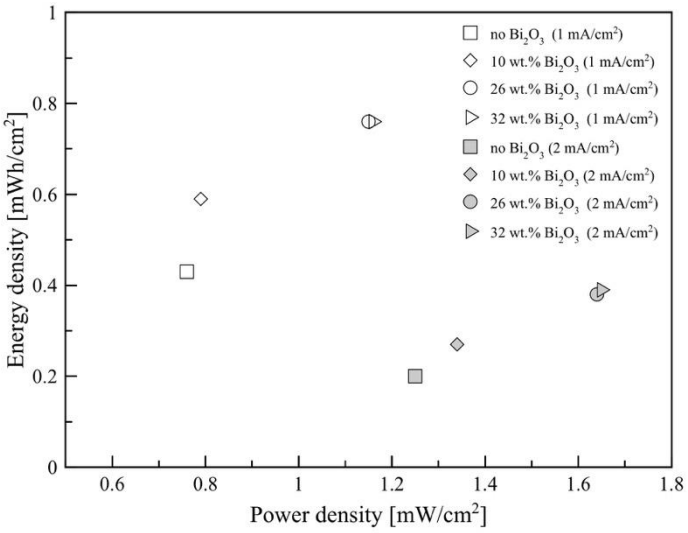

Fig. 7. Ragone diagram of the batteries using carbon black and various wt.% of Bi_2O_3: no Bi_2O_3 (54.26 Zn, 5.71 ZnO, 1.25 SBD, 38.77 C, wt.% dry basis), 10 wt.% Bi_2O_3 (39.10 Zn, 4.12 ZnO, 0.90 SBD, 27.94 C, 27.94 Bi_2O_3, wt.% dry basis), 26 wt.% Bi_2O_3 (25.69 Zn, 2.70 ZnO, 0.59 SBD, 18.35 C, 52.66 Bi_2O_3, wt.% dry basis) and 32 wt.% Bi_2O_3 (21.77 Zn, 2.29 ZnO, 0.50 SBD, 15.55 C, 59.88 Bi_2O_3, wt.% dry basis).

Figure 7 shows the Ragone plot of the batteries using carbon black and Bi_2O_3 at various concentrations. The Ragone plot shows the relationship between energy density and power density at current densities of 1.0 mA/cm^2 and 2.0 mA/cm^2. The energy density shows how much energy is available, while the power density present show fast the energy can be discharged. As power density increases, the energy density significantly decreases. By increasing the content of Bi_2O_3, both energy and current densities of the batteries were improved. However, the improvement reached the limit at 26 wt.% Bi_2O_3. As previously discussed, immoderate loading of Bi_2O_3 lowers the zinc content, which is the main reactant in zinc dissolution reaction.

4. Conclusion

This work highlighted the improvement of electrochemical performance for flexible printed zinc-air batteries. The use of additive materials including carbon black, Na_2SiO_3 and Bi_2O_3 for implementation on the anode was investigated. The addition of carbon black is an effective method to improve electronic conductivity of the anode. Again, when Bi_2O_3 or Na_2SiO_3 were introduced, the batteries performed better. Bi_2O_3 and Na_2SiO_3 contributed in inhibiting passivation of zinc active surfaces and provides effective electrolyte access. Overall, Bi_2O_3 and Na_2SiO_3 facilitated the transport of hydroxide ions across multilayers of zinc particles, including those which do not directly contact with the electrolyte. Thus, the printed zinc-air batteries show higher performance and more promise for future electronic devices. Moreover, the addition of these additives can be extended to the application for other zinc-ion batteries.

Acknowledgments

The Higher Education Research Promotion and National Research University Project of Thailand, Office of the Higher Education Commission (NRU-59-051-EN) and The Institutional Research Grant (Chulalongkorn University, RES-57-411-21-076 and The Thailand Research Fund, IRG-5780014) are acknowledged. T.Y. thanks the partial support from Hokkaido University and Canon Foundation. S.K. thanks Hokkaido University for the financial support for his stay in Sapporo.

References

[1] A. C. Siegel, S. T. Phillips, M. D. Dickey, N. Lu, Z. Suo, and G. M. Whitesides, "Foldable printed circuitboards on paper substrates," *Adv. Funct. Mater.*, vol. 20, no. 1, pp. 28–35, 2010.

[2] G. Grau, J. Cen, H. Kang, R. Kitsomboonloha, W. J. Scheideler, and V. Subramanian, "Gravure-printedelectronics: Recent progress in tooling development, understanding of printing physics, and realization ofprinted devices," *Flex. Printed Elec.*, vol. 1, no. 2, p. 023002, Jun. 2016.

[3] S. Park, M. Vosguerichian, and Z. Bao, "A review of fabrication and applications of carbon nanotube film-based flexible electronics," *Nanoscale*, vol. 5, pp. 1727–1752, 2013.

[4] N. Panuthai, R. Savanglaa, P. Praserthdam, and S. Kheawhom, "Characterization of copper-zinc nanoparticles synthesized via submerged arc discharge with successive reduction process," *Jpn. J. Appl. Phys.*, vol. 53, pp. 05HA11–1 – 05HA11–6, 2014.

[5] S. Suren, W. Limkitnuwat, P. Benjapongvimon, and S. Kheawhom, "Conductive film by spray pyrolysis of self-reducing copper-silver amine complex solution," *Thin Solid Films*, vol. 607, pp. 36–42, May 2016.

[6] K. Wongrujipairoj, L. Poolnapol, A. Arpornwichanop, S. Suren, and S. Kheawhom, "Suppression of zinc anode corrosion for printed flexible zinc-air battery," *Phys. Status Solidi B*, vol. 254, no. 2, pp.1600442-1–1600442-6, 2017.

[7] A. M. Gaikwad, D. A. Steingart, and T. N. Ng, "A flexible high potential printed battery for powering printed electronics," *Appl. Phys. Lett.*, vol. 102, no. 23, p. 233302, 2013.

[8] W. Lao-atiman, T. Julaphatachote, P. Boonmongkolras, and S. Kheawhom, "Printed Transparent Thin Film Zn-MnO_2 Battery," *J. Electrochem. Soc.*, vol. 164, no. 4, pp. A859–A863, Feb. 2017.

[9] S. Kim, K. Choi, S. Cho, S. Choi, S. Park, and S. Lee, "Printable solid-state lithium-ion batteries: A newroute toward shape-conformable power sources with aesthetic versatility for flexible electronics," *NanoLett.*, vol. 15, no. 8, pp. 5168–5177, 2015.

[10] K. T. Braam, S. K. Volkman, and V. Subramanian, "Characterization and optimization of a printed, primarysilver-zinc battery," *J. Power Sources*, vol. 199, pp. 367–372, Feb. 2012.

[11] S. Suren and S. Kheawhom, "Development of a High Energy Density Flexible Zinc-Air Battery," *J. Electrochem. Soc.*, vol. 163, no. 6, pp. A846–A850, Jan. 2016.

[12] D. U. Lee, H. W. Park, D. Higgins, L. Nazar, and Z. Chen, "Highly active graphene nanosheets prepared via extremely rapid heating as efficient zinc-air battery electrode material," *J. Electrochem. Soc.*, vol. 160, no. 9, pp. F910–F915, 2013.

[13] M. N. Masri and A. A. Mohamad, "Effect of adding carbon black to a porous zinc anode in a zinc-air battery," *J. Electrochem. Soc.*, vol. 160, no. 4, pp. A715–A721, 2013.

[14] F. W. Thomas Goh, Z. Liu, T. S. A. Hor, J. Zhang, X. Ge, Y. Zong, A. Yu, and W. Khoo, "A near-neutral chloride electrolyte for electrically rechargeable zinc-air batteries," *J. Electrochem. Soc.*, vol. 161, no. 14, pp. A2080–A2086, 2014.

[15] N. Shaigan, W. Qu, and T. Takeda, "Morphology control of electrodeposited zinc from alkaline zincate solutions for rechargeable zinc-air batteries," *ECS Trans.*, vol. 28, pp. 35–44, 2010.

[16] J. Chen and F. Cheng, "Combination of lightweight elements and nanostructured materials for batteries," *Acc. Chem. Res.*, vol. 42, no. 6, pp. 713–723, 2009.

[17] S.-W. Eom, C.-W. Lee, M.-S. Yun, and Y.-K. Sun, "The roles and electrochemical characterizations of activated carbon in zinc-air battery cathodes," *Electrochim. Acta*, vol. 52, no. 4, pp. 1592 – 1595, 2006.

[18] S.-M. Lee, Y.-J. Kim, S.-W. Eom, N.-S. Choi, K.-W. Kim, and S.-B. Cho, "Improvement in self-discharge of Zn anode by applying surface modification for Zn-air batteries with high energy density," *J. Power Sources*, vol. 227, pp. 177 – 184, 2013.

[19] H. S. Kim, Y. N. Jo, W. J. Lee, K. J. Kim, and C. W. Lee, "Coating on zinc surface to improve the electrochemical behavior of zinc anodes for zinc-air fuel cells," *Electroanalysis*, vol. 27, no. 2, pp. 517–523, 2015.

[20] C. W. Lee, K. Sathiyanarayanan, S. W. Eom, and M. S. Yun, "Novel alloys to improve the electrochemicalbehavior of zinc anodes for zinc/air battery," *J. Power Sources*, vol. 160, no. 2, pp. 1436–1441, 2006.

[21] Y. N. Jo, H. S. Kim, K. Prasanna, P. R. Ilango, W. J. Lee, S. W. Eom, and C. W. Lee, "Effect of additives on electrochemical and corrosion behavior of gel type electrodes for Zn-air system," *Ind. Eng. Chem. Res.*, vol. 53, no. 44, pp. 17370–17375, 2014.

[22] P. Li, C. Hu, T. Lee, W. Chang, and T. Wang, "Synthesis and characterization of carbon black/manganeseoxide air cathodes for zinc-air batteries," J. Power Sources, vol. 269, pp. 88–97, 2014.
[23] M. Hilder, B. Winther-Jensen, and N. Clark, "Paper-based, printed zinc-air battery," *J. Power Sources*, vol. 194, no. 2, pp. 1135–1141, 2009.
[24] M. Hilder, B. Winther-Jensen, and N. B. Clark, "The effect of binder and electrolyte on the performance ofthin zinc-air battery," *Electrochim. Acta*, vol. 69, pp. 308–314, 2012.
[25] R. Othman, A. Yahaya, and A. Arof, "A zinc-air cell employing a porous zinc electrode fabricated fromzinc–graphite-natural biodegradable polymer paste," *J. Appl. Electrochem.*, vol. 32, no. 12, pp. 1347–1353, 2002.
[26] C. W. Lee, S. W. Eom, K. Sathiyanarayanan, and M. S. Yun, "Preliminary comparative studies of zinc andzinc oxide electrodes on corrosion reaction and reversible reaction for zinc/air fuel cells," *Electrochim. Acta*, vol. 52, no. 4, pp. 1588–1591, 2006.
[27] G. Wu, S. Lin, and C. Yang, "Alkaline Zn-air and Al-air cells based on novel solid PVA/PAA polymer electrolyte membranes," *J. Membr. Sci.*, vol. 280, no. 1–2, pp. 802–808, 2006.
[28] M. N. Masri, M. F. M. Nazeri, C. Y. Ng, and A. A. Mohamad, "Tapioca binder for porous zinc anodeselectrode in zinc-air batteries," *J. King Saud Univ. Sci.*, vol. 27, no. 2, pp. 217–224, 2015.
[29] A. R. Mainar, O. Leonet, M. Bengoechea, I. Boyano, I. de Meatza, A. Kvasha, A. Guerfi, and J. Alberto Blázquez, "Alkaline aqueous electrolytes for secondary zinc-air batteries: An overview," *Int. J. Energy. Res.*, vol. 40, no. 8, pp. 1032–1049, 2016.
[30] L. Gui, Y. Ling, G. Li, Z. Wang, Y. Wan, R. Wang, B. He, and L. Zhao, "Enhanced sinterability and conductivity of $BaZr_{0.3}Ce_{0.5}Y_{0.2}O_3$-δ by addition of bismuth oxide for proton conducting solid oxide fuel cells," *J. Power Sources*, vol. 301, pp. 369–375, 2016.
[31] W. Fang, N. Zhang, L. Fan, and K. Sun, "The facile preparation of a carbon coated Bi_2O_3 nanoparticle/nitrogen-doped reduced graphene oxide hybrid as a high-performance anode material for lithium-ion batteries," *RSC Adv.*, vol. 6, pp. 99825–99832, 2016.
[32] J. Shin, J.-M. You, J. Z. Lee, R. Kumar, L. Yin, J. Wang, and Y. Shirley Meng, "Deposition of ZnO on bismuth species towards a rechargeable Zn-based aqueous battery," *Phys. Chem. Chem. Phys.*, vol. 18, pp. 26376–26382, 2016.
[33] W. K. Zhang, X. Y. Tao, H. Huang, S. J. Gu, and Y. P. Gan, "ZnO/ZnO-Bi_2O_3 nanocomposite as an anode material for Ni-Zn rechargeable battery," *Advanced Materials Research*, vol. 396, pp. 1725–1729, 2012.
[34] F. Moser, F. Fourgeot, R. Rouget, O. Crosnier, and T. Brousse, "In situ X-ray diffraction investigation of zinc based electrode in Ni–Zn secondary batteries," *Electrochim. Acta*, vol. 109, pp. 110–116, 2013.
[35] M. McKubre and D. D. Macdonald, "The dissolution and passivation of zinc in concentrated aqueous hydroxide," *J. Electrochem. Soc.*, vol. 128, no. 3, pp. 524–530, 1981.
[36] R. W. Powers and M. W. Breiter, "The anodic dissolution and passivation of zinc in concentrated potassium hydroxide solutions," *J. Electrochem. Soc.*, vol. 116, no. 6, pp. 719–729, Jun. 1969.
[37] N. Sammes, G. Tompsett, H. Näfe, and F. Aldinger, "Bismuth based oxide electrolytes-structure and ionic conductivity," *J. Eur. Ceram. Soc.*, vol. 19, no. 10, pp. 1801–1826, 1999.